1   Preface

1.1   Context

1.2   Acknowledgements

1.3   Contact Me

2   Code Usage

2.1   Code Structure

2.2   Running Scripts

3   Morris-Lecar Neuron

This project investigated the Morris-Lecar model of a neuron. This section goes over background theory on the model.

3.1   Circuit Model

The Morris-Lecar description [3] models a neuron as having a membrane potential v, defined to be the difference in voltage between the inside and outside of the neuron cell. Current flows through potassium and calcium channels in the membrane, labelled as I_K and I_{Ca}, respectively. There is also some current arising form other ions, which is collectively totalled as the leak current I_L. The combined potassium, calcium, and leak channels each have an effective conductance (or, taking reciprocals, resistance) and potential. Finally, the membrane has a capacitance C. **Figure 3.1** depicts a circuit for this model.

Consequently, the membrane potential obeys the following first order differential equation:

$$C\frac{dv}{dt} = I - g_K(v - V_K) - g_{Ca}(v - V_{Ca}) - g_L(v - V_L) \tag{3.1}$$

Nominally, the potassium and calcium conductances are non-constant. Rather, they obey the following equations:

$$g_K = \bar{g}_K w \tag{3.2}$$
$$g_{Ca} = \bar{g}_{Ca} m \tag{3.3}$$
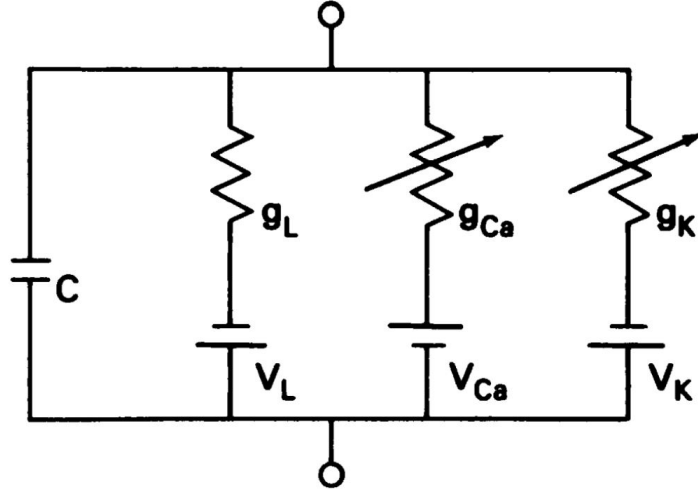
where $\bar{g}_K, \bar{g}_{Ca}$ are constant.

Figure 3.1: TODO + cite ML

At constant v, the parameters $x = w, m$ are governed by first order differential equations of the following form:

$$\frac{dx}{dt} = \lambda_x(v)(x_\infty(v) - x) \tag{3.4}$$

However, the m timescale is much shorter than the w timescale, so that $m \approx m_\infty(v)$ in (3.1). Furthermore, to be consistent with [2], we may re-arrange the $x = w$ version of (3.4) to be of the following form:

$$\frac{dw}{dt} = \alpha(v)(1 - w) - \beta(v)w \tag{3.5}$$

where

$$\alpha(v) = \frac{1}{2}\phi \cosh\left(\frac{v - V_3}{2V_4}\right)\left(1 + \tanh\left(\frac{v - V_3}{V_4}\right)\right) \tag{3.6}$$

$$\beta(v) = \frac{1}{2}\phi \cosh\left(\frac{v - V_3}{2V_4}\right)\left(1 - \tanh\left(\frac{v - V_3}{V_4}\right)\right) \tag{3.7}$$

Furthermore, we have

$$m_\infty(v) = \frac{1}{2}\left(1 + \tanh\left(\frac{v - V_1}{V_2}\right)\right) \tag{3.8}$$

3.2   Morris-Lecar Parameters

The parameters from [2] used in this project are given in **Table 3.1**. Sometimes I and/or *phi* are varied to assess the bifurcational behaviuor of the system.

Variable	Value	Units
C	20	$\mu F/cm^2$
g_L	2.0	mS/cm^2
$\bar{g}_{Ca}$	4.4	mS/cm^2
$\bar{g}_K$	8	mS/cm^2
V_L	-60	mV
V_{Ca}	120	mV
V_K	-84	mV
V_1	-1.2	mV
V_2	18.0	mV
V_3	2.0	mV
V_4	30.0	mV
ϕ	0.04	ms^{-1}
I	90	$\mu A/cm^2$

Table 3.1: TODO

3.3 Helpful Resources

TODO

4   Dynamics

4.1   Bautin Bifurcation

Consider a 2-dimensional dynamical system $(x(t), y(t)) \in \mathbb{R}^2$. We may equivalently define the complex variable $z = x + iy \in \mathbb{C}$. Alternatively, we may express this system in polar coordinates: $z = re^{i\varphi}$. Now, let us consider the system

$$\frac{dz}{dt} = \lambda z \left(1 + k_1 |z|^2 + k_2 |z|^4 + O\left(|z|^5\right)\right) \tag{4.1}$$

$$= \lambda z + c_1 z |z|^2 + c_2 z |z|^4 + O\left(|z|^6\right) \tag{4.2}$$

Here $c_j = \lambda k_j$, and $\lambda, c_j \in \mathbb{C}$ for $j = 1, 2$. Let us rewrite $\lambda = \alpha + i\omega, c_j = l_j + im_j$, where $\alpha, \omega, l_j, m_j \in \mathbb{R}$. Then taking real and imaginary parts of (4.2) gets us

$$\frac{dx}{dt} = (\alpha + l_1 r^2 + l_2 r^4)x - (\omega + m_1 r^2 + m_2 r^4)y \tag{4.3}$$

$$\frac{dy}{dt} = (\omega + m_1 r^2 + m_2 r^4)x + (\alpha + l_1 r^2 + l_2 r^4)y \tag{4.4}$$

Here we dropped terms of order $O\left(|z|^6\right)$ or higher. We do so by assuming that $l_2 < 0$ (and is thus nonzero). The parameter l_2, known as the *second Lyapunov coefficient*, is indeed negative for the Morris-Lecar neuron (as we shall discuss later). Doing some calculus, the equations for r and φ become:

$$\frac{dr}{dt} = r(\alpha + l_1 r^2 + l_2 r^4) \tag{4.5}$$

$$\frac{d\varphi}{dt} = \omega + m_1 r^2 + m_2 r^4 \tag{4.6}$$

We see that there is a fixed point at $r = 0$. Furthermore, there are circular limit cycles at r^2 satisfying the quadratic

$$f(r^2) = r^4 + \frac{l_1}{l_2} r^2 + \frac{\alpha}{l_2} = 0 \tag{4.7}$$

Since these limit cycles occur at $r > 0$, we have precisely one limit cycle for each r^2 root. The discriminant Δ of the quadratic (4.7) is

$$\Delta = \left(\frac{l_1}{l_2}\right)^2 - 4\frac{\alpha}{l_2} = \frac{1}{l_2^2}\left(l_1^2 - 4\alpha l_2\right) \tag{4.8}$$

The sign of Δ is therefore just the sign of $l_1^2 - 4\alpha l_2$. Then a necessary condition for there to be limit cycles i.e. positive real roots for r^2 is:

$$\alpha \geq \frac{l_1^2}{4l_2} \tag{4.9}$$

Now assuming that $\Delta \geq 0$ i.e. the roots for r^2 are all real, we use Vieta's formulas to note that the sum and product of the roots are $-\frac{l_1}{l_2}, \frac{\alpha}{l_2}$, repsectively.

For $\Delta \geq 0$, exactly one positive root exists precisely when $\alpha > 0 \therefore \frac{\alpha}{l_2} < 0$. But we immediately have $\alpha > 0 \geq \frac{l_1}{4l_2}$, satisfying the discriminant condition.

Now if $\alpha = 0$, then at least one root must coincide with $r = 0$. The other root is thus equal to $-\frac{l_1}{l_2}$ and is positive iff $l_1 > 0$.

Next, if $\alpha < 0$, both roots have the same sign. If $l_1 \leq 0$ then the sum of the roots is nonpositive, resulting in both roots being nonpositive. Thus there are no limit cycles for $\alpha < 0, l_1 \leq 0$. However, if $\alpha < 0$ and $l_1 > 0$, there are two positive roots for r^2 if $\alpha > \frac{l_1^2}{4l_2}$. If instead, $l_1 > 0$ and $\alpha = \frac{l_1^2}{4l_2} < 0$ then there is a repeated positive root and therefore one limit cycle.

Finally, the stability of the limit cycles and $r = 0$ fixed point is determined by the sign of $f(r^2)$ in between these roots. Since $l_2 < 0$, the outermost limit cycle (or fixed point if none
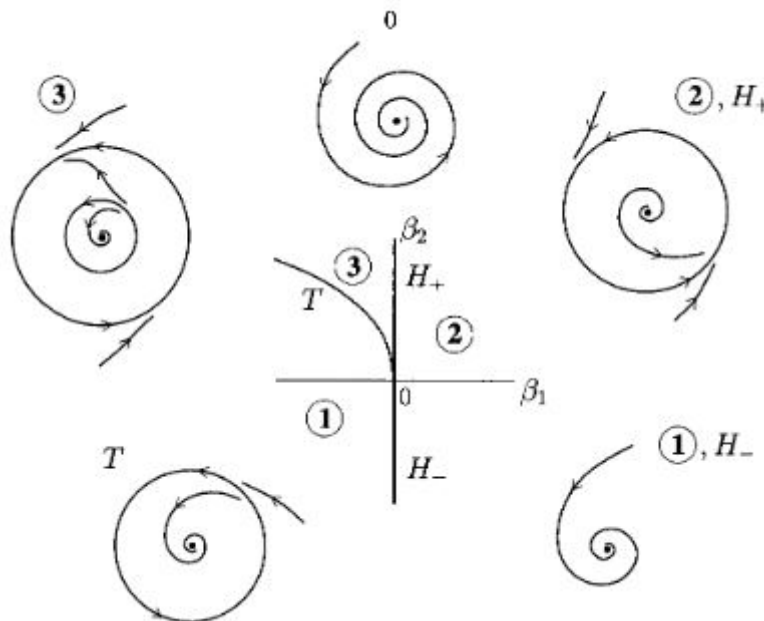
Figure 4.1: TODO + cite Kunetzsov

exists) attracts from $r = \infty$. Meanwhile, the stability of the fixed point is determined by the sign of α (or l_1 if $\alpha = 0$, or $l_2 < 0$ if $\alpha, l_1 = 0$). Finally, if there are two limit cycles, the inner one is unstable while the outer one is stable since $f(r^2)$ is a downwards parabola in r^2.

Put all together, the bifurcation diagram is given in **Figure 4.1**

The curve $H_- = \{\alpha = 0, l_1 < 0\}$, in **Figure 4.1** is a *Hopf bifurcation*. For a fixed $l_1 < 0$, varying α near zero affects the stability of the system; $\alpha < 0$ has a limit cycle whereas $\alpha > 0$ does not. Similarly, $H_+ = \{\alpha = 0, l_1 > 0\}$ is also a Hopf bifurcation. This time, a limit cycle is produced at the fixed point when varying $\alpha > 0$ to $\alpha < 0$. In general, the Hopf bifurcation is a local codim-1 bifurcation, where a limit cycle appears from/disappears into a fixed point.

The curve $T = \{l_1 > 0, \alpha = \frac{l_1^2}{4l_2}\}$ is a *saddle node of limit cycles (SNLC) bifurcation*. Here the two limit cycles in region 3 collapse into a single limit cycle on T. Varying a parameter more (e.g. decreasing α or l_1) will cause the semi-stable limit cycle to disappear. Like the Hopf bifurcation, the SNLC bifurcation is a local codim-1 bifurcation.

Finally, a *Bautin bifurcation* occurs near the point $\alpha, l_1 = 0$ in this model system. Since two parameters are varied in this bifurcation (α, l_1), this is a local codim-2 bifurcation.

4.2   Morris-Lecar Dynamics

4.3   Scaling Results

4.4   Helpful Resources

5   Stochastics

5.1   Itô Calculus

X_t is a *Wiener process* iff it is a continuous-time stochastic process satisfying the following conditions:

1. **Stationary increments:** If $s \leq t$, $X_t - X_s$ has the same distribution as $X_{t-s} - X_0$.

2. **Independent increments:** If $s \leq t$, $X_t - X_s$ is independent of X_r for all $r \leq s$.

3. **Continuous paths:** X_t is a continuous function of t.

Here, a Wiener process is characterized by three paramters: the initial condition X_0, the drift m, and the variance parameter σ^2. For $s \leq t$, the increment $X_t - X_s$ is distributed as a Gaussian with mean $m(t-s)$ and variance $\sigma^2(t-s)$:

$$X_t - X_s \sim N\left(m(t-s), \sigma^2(t-s)\right) \tag{5.1}$$

The *standard* Wiener process B_t has $B_0 = 0$, $m = 0$, and $\sigma^2 = 1$. We may therefore write

$$dX_t = m\,dt + \sigma\,dB_t \tag{5.2}$$

Note that dB_t is distributed as

$$dB_t \sim \sqrt{dt}\,Z \tag{5.3}$$

where Z is a standard normal random variable. Now in general, if f is a function of X_t, then we may write

$$df(X_t) = g(X_t)dt + h(X_t)dB_t \tag{5.4}$$

for some functions $g(X_t), h(X_t)$ (Itô's lemma gives a more precise result, but we will not utilize it for these purposes).

The n-dimensional standard Wiener process $\mathbf{B_t}$ is simply a vector of n independent standard Wiener processes. Then an n-dimensional dyanmical system $\mathbf{X}$ can be expressed in the form

$$d\mathbf{X} = \mathbf{g}(\mathbf{X})dt + \mathbf{H}(\mathbf{X})\mathbf{dB_t} \tag{5.5}$$

Here $\mathbf{g}$ is a vector while $\mathbf{H}$ is a matrix.

5.2 Stochastic Morris-Lecar

We can model the neuron as having N_K potassium channels (in this project, we are typically on the order of $N_K \sim 1000$), each of which can be fully open or closed. The opening rate (i.e. probability rate of transition from the closed state to the open state) and closing rate for each channel would be $\alpha(v)$ and $\beta(v)$ from (3.5), respectively. Then over a small time increment dt, the probability of a closed channel opening is $\alpha(v)dt$. Likewise, the probability of an open channel closing is $\beta(v)dt$.

Over a time increment of dt, we have

$$dw = w(t + dt) - w(t) \sim \frac{\text{Binom}\left(N_K(1 - w), \alpha dt\right) - \text{Binom}\left(N_K w, \beta dt\right)}{N_K} \tag{5.6}$$

Note that $\text{Binom}\,(n, p, =) \sum_{j=1}^{n} I_j$, where each I_j is an independent indicator random variable with probability p. By the central limit theorem, when n is large

$$\text{Binom}\,(n, p) \sim np + \sqrt{np(1 - p)}Z \tag{5.7}$$

where Z is a standard normal random variable. Then (5.6) becomes

$$dw \sim \frac{\left(N_K(1 - w)\alpha dt + \sqrt{N_K(1 - w)\alpha dt(1 - \alpha dt)}Z_1\right) - \left(N_K w\beta dt + \sqrt{N_K w\beta dt(1 - \beta dt)}Z_2\right)}{N_K} \tag{5.8}$$

Here Z_1 and Z_2 are independent normal random variables. This is because the closed and open channels are independent (as we assumed all the channels to be independent). Since dt is small, $1 - \alpha dt \approx 1$. So

$$dw \sim (\alpha(1 - w) - \beta w)\,dt + \frac{1}{\sqrt{N_K}}\sqrt{\alpha(1 - w) + \beta w}\sqrt{dt}Z \tag{5.9}$$

As a system of stochastic differential equations, we have

$$\begin{pmatrix} v \\ w \end{pmatrix}' = \begin{pmatrix} f(v, w) \\ g(v, w) \end{pmatrix} dt + \begin{pmatrix} 0 & 0 \\ 0 & h(v, w) \end{pmatrix} \mathbf{dB_t} \tag{5.10}$$

$$f(v, w) = \frac{I - \bar{g}_K w(v - V_K) - \bar{g}_{Ca} m_\infty(v)(v - V_{Ca}) - g_L(v - V_L)}{C} \tag{5.11}$$

$$g(v, w) = \alpha(v)(1 - w) - \beta(v)w \tag{5.12}$$

$$h(v, w) = \frac{1}{\sqrt{N_K}}\sqrt{\alpha(v)(1 - w) + \beta(v)w} \tag{5.13}$$

5.3 Euler-Maruyama Method

The Euler-Maruyama method is a generalization of the Euler method to stochastic differential equations of the form (5.5). Here, a small finite time increment dt is chosen.

Then, starting from an initial condition $\mathbf{X}(0)$, we iteratively compute

$$\mathbf{X}(t + dt) = \mathbf{X}(t) + \mathbf{g}(\mathbf{X})dt + \mathbf{H}(\mathbf{X})\mathbf{Z}\sqrt{dt} \qquad (5.14)$$

Here $\mathbf{Z}$ is a randomly generated vector, where each entry is obtained from an independent unit normal distribution. The resulting path $\mathbf{X}(t)$ will be distributed approximately as the true distribution; thus, many trials of the Euler-Maruyama method can be used to obtain statistics for the process (e.g. interspike intervals, which will be discussed later).

To ease computations, only the second entry of $\mathbf{Z}$ needs to be generated for the 2-dimensional stochastic Morris-Lecar model (since only $\mathbf{H_{22}}$ is nonzero). Furthermore, the random numbers can all be generated at the start rather than at every iteration.

5.4   Helpful Resources

6   Interspike Intervals

6.1   Defining Intervals

6.2   Results

7   Poincare-Like Maps

8   Alternative Dynamics

8.1   Jacobi Dynamics

Physically, w should be bounded in $[0, 1]$. However, the equations described in (5.10)-(5.13) imply a finite (albeit small) possibility of w being outside of $[0, 1]$. *In practice*, this issue never really manifests. For theoretical satisfaction, however, we may instead use–for a fixed v–a bounded diffusion process for w.

Following [1], we choose the simplest diffusion process that mimics the system. Arguably, we wish to preserve the dynamic part $g(v, w)$ while having as simple of a variance coefficient $h(v, w)^2$ as possible. The preservation of $g(v, w)$ can be vouched for as it, loosely speaking, determines the "average" behaviour of the system, as well as defining the $N_K \to 0$ limit behaviour. Seeing that $g(v, w)$ is linear in w, we consider Pearson diffusions, where $h(v, w)^2$ is a polynomial of degree at most two. It turns out that the Jacobi diffusion is the only Pearson diffusion bounded in a finite interval. This renders a Jacobi diffusion as the "simplest" bounded diffusion process appropriate for the stochastic Morris-Lecar system.

We follow the discussion [1] on the Jacobi diffusion here. The Jacobi diffusion bounded on $(0, 1)$ has the form (for fixed v)

$$dw = -\theta(w - \mu)dt + \gamma\sqrt{2\theta w(1 - w)}dB_t \tag{8.1}$$

Equating the dynamic part gets us

$$\theta = \alpha + \beta, \quad \mu = \frac{\alpha}{\alpha + \beta} \tag{8.2}$$

Note that we necessarily have $\alpha(v), \beta(v) \geq 0$ as can be seen from (3.6)-(3.7). The Jacobi diffusion is *ergodic* for

$$\gamma^2 \leq \mu, 1 - \mu \tag{8.3}$$

To retain this property, we can rewrite $\gamma = \sigma^*\delta(v)$, where σ^* is a constant that can be fit (to e.g. match $h(v, w)$ at the fixed point) and $\delta(v)$ is a simple function of v. Of course, such a choice of $\sigma^*, \delta(v)$ is not unique since we can rewrite $\sigma^* \mapsto x\sigma^*$, $\delta(v) \mapsto \frac{\delta(v)}{x}$ for any nonzero x. We therefore assert the condition that $\sigma^* \in [0, 1]$ and that (8.3) holds for all σ^* in that range. When fitting σ^*, the ergodicity requirement becomes verifying that $\sigma^* \in [0, 1]$.

γ^2 is largest when $\sigma^* = 1$, so our task becomes assuring that $\delta(v)^2 \leq \mu, 1 - \mu$ i.e.

$$\delta(v)^2 \leq \frac{\alpha(v)}{\alpha(v) + \beta(v)}, \frac{\beta(v)}{\alpha(v) + \beta(v)} \tag{8.4}$$

Naively, we could define

$$\delta(v) = \sqrt{\min\left(\frac{\alpha(v)}{\alpha(v) + \beta(v)}, \frac{\beta(v)}{\alpha(v) + \beta(v)}\right)} \tag{8.5}$$

However, the piecewise definition comes at the cost of differentiability. To make $\delta(v)$ analytically "well-behaved", we instead define $\delta(v)^2$ to be the harmonic sum of $\mu, 1 - \mu$ (as is done for e.g. parallel resistors):

$$\delta(v)^2 = \frac{\mu(1 - \mu)}{\mu + (1 - \mu)} = \frac{\alpha\beta}{\alpha + \beta} \tag{8.6}$$

Thus

$$\gamma = \sigma^*\sqrt{\frac{\alpha\beta}{\alpha + \beta}} \tag{8.7}$$

Equation (8.1) now becomes

$$dw = (\alpha(v)(1 - w) - \beta(v)w)dt + \sigma^*\sqrt{2\frac{\alpha(v)\beta(v)}{\alpha(v) + \beta(v)}w(1 - w)}dB_t \tag{8.8}$$

The fixed point of the system occurs at approximately $(v_{eq}, w_{eq}) = (-26.6, 0.129)$. Plugging this into (5.13) and the coefficient in front of dB_t in (8.8) gives

$$h(v_{eq}, w_{eq}) = \frac{0.1003}{\sqrt{N_K}} = 0.03365\sigma^* \tag{8.9}$$

That gives us

$$\sigma^* = \frac{2.98}{\sqrt{N_K}} \tag{8.10}$$

Since N_K is on the order of 1000, and certainly larger than 9, we see that typical fits of σ^* are indeed ergodic.

8.2 Linearized Dynamics

Near the fixed point, we can expand (5.10) as a linear model as in [1]. Since the deterministic part is zero to zeroth order, we expand it to first order. In contrast, the stochastic part $h(v, w)$ is nonzero to zeroth order, so we need only expand that to zeroth order. That gets us

$$\begin{pmatrix} v \\ w \end{pmatrix}' \approx \mathbf{M} \begin{pmatrix} v \\ w \end{pmatrix} dt + \begin{pmatrix} 0 \\ \frac{0.1003}{\sqrt{N_K}} dB_t \end{pmatrix} \tag{8.11}$$

Here we used the value of (8.9) for the stochastic part. Meanwhile, $\mathbf{M}$ is the Jacobian matrix of the dynamic part in (5.10):

$$\mathbf{M} = D \begin{pmatrix} f(v, w) \\ g(v, w) \end{pmatrix} \tag{8.12}$$

The linear approximation is valid in a small region near the fixed point. Of course, this region is necessarily within the unstable limit cycle. Numerical experiemnts can provide more clarity into the size of this region. Such a region would be elliptical, however. This is because the coordinates v, w are not symmetrical in the sense that $\mathbf{M}$ does not stretch and shear them uniformly. To remove this complication and simplify the equation, we can define the matrix

$$\mathbf{Q} = \begin{pmatrix} \omega & m_{11} + \lambda \\ 0 & m_{21} \end{pmatrix} \tag{8.13}$$

Then we define

$$\mathbf{A} = \mathbf{Q}^{-1}\mathbf{M}\mathbf{Q} = \begin{pmatrix} -\lambda & \omega \\ -\omega & -\lambda \end{pmatrix} \tag{8.14}$$

$$\tilde{\mathbf{x}} = \mathbf{Q}^{-1} \begin{pmatrix} v \\ w \end{pmatrix} \tag{8.15}$$

$$\mathbf{c} = \mathbf{Q}^{-1} \begin{pmatrix} 0 \\ \frac{0.1003}{\sqrt{N_K}} dB_t \end{pmatrix} \tag{8.16}$$

We then obtain the symmetrized equation

$$d\tilde{\mathbf{x}} = \mathbf{A}\tilde{\mathbf{x}} + \mathbf{c} \tag{8.17}$$

In the transformed space $\tilde{\mathbf{x}}$, it makes sense to talk about circular regions as opposed to elliptical regions in the original coordinate system. Finally, we can further simplify this equation by factoring out rotations. If we define

$$\tilde{\tilde{\mathbf{x}}} = R_{\omega t}\tilde{\mathbf{x}} = \begin{pmatrix} \cos\omega t & -\sin\omega t \\ \sin\omega t & \cos\omega t \end{pmatrix} \tilde{\mathbf{x}} \tag{8.18}$$

Then we obtain the equation

$$d\tilde{\tilde{\mathbf{x}}} = -\lambda\tilde{\tilde{\mathbf{x}}} + R_{\omega t}\mathbf{c} \tag{8.19}$$

8.3   Numerical Comparison

8.4   Helpful Resources

9   Patched Model

10   Next Steps

References

[1] Susanne Ditlevsen and Priscilla Greenwood. The morris–lecar neuron model embeds a leaky integrate-and-fire model. *Journal of mathematical biology*, 67(2):239–259, 2013;2011;.

[2] Priscilla E. Greenwood, Lawrence M. Ward, SpringerLink (Online service), SpringerLINK ebooks Mathematics, and Statistics. *Stochastic Neuron Models*, volume 1.5. Springer International Publishing, Cham, 1st 2016. edition, 2016.

[3] C. Morris and H. Lecar. Voltage oscillations in the barnacle giant muscle fiber. *Biophysical journal*, 35(1):193–213, 1981.